Resonance energy transfers in the induction phenomenon in quartic Fermi-Pasta-Ulam chains

G. Christie and B. I. Henry
Department of Applied Mathematics, University of New South Wales, Sydney, New South Wales 2052, Australia
(Received 25 February 1998; revised manuscript received 20 April 1998)

We have reexamined the induction phenomenon in quartic Fermi-Pasta-Ulam chains whereby an initially excited harmonic mode transfers energy apparently abruptly to other harmonic modes after the elapse of an initial induction time. The previous explanation for this phenomenon using the Mathieu function stability analysis is shown to be unsatisfactory. An analysis using a shifted frequency perturbation scheme and the analysis of mode resonances correctly identifies the initial pattern of mode excitation and the dominant modes in the induction phenomenon. [S1063-651X(98)04009-4]

PACS number(s): 05.45.+b, 63.70.+h, 63.90.+t

I. INTRODUCTION

The Fermi-Pasta-Ulam (FPU) chain [1] of N equimass particles coupled by linear and nonlinear nearest-neighbor forces is a paradigm for studying fundamental problems in the foundations of statistical mechanics such as ergodicity and equipartition of energy in solids [2]. In the absence of the nonlinear forces the chain dynamics is equivalent to a set of independent linear oscillators, each with different frequency (harmonic modes). The central focus of studies of FPU chains has been the distribution of the system energy among the harmonic modes. Phase space averages for the linear chain yield equipartition of energy: equal energy content in each harmonic mode. On the other hand, since there is no coupling between the harmonic modes in a linear chain, time averages simply yield the initial energy distribution among the modes that is not uniform for generic initial conditions.

With the inclusion of nonlinear forces the harmonic modes can redistribute energy among themselves; however, calculations of phase space averages and time averages are generally algebraically intractable and comparisons between the two require numerical simulations. Early numerical studies of the FPU model revealed two contrasting behaviors. In the original computer experiments of Fermi, Pasta, Tsingou, and Ulam [1] energy was initially supplied to the lowest-frequency harmonic mode. The energy did not become uniformly distributed among the other harmonic modes of the system but instead varied periodically (the FPU period). In a subsequent experiment by Ooyama, Hirooka, and Saitô [3] (see also [4,5]) energy was initially supplied to a high-frequency harmonic mode (mode 11) in a FPU chain with 15 movings particles. In this study it was reported that above a threshold value of the nonlinear coupling parameter the energy remained in the initially excited mode over an initial induction time before it was abruptly transferred to other harmonic modes.

The results of these and other numerical studies of FPU chains have been explained qualitatively by appealing to the Kolmogorov-Arnol'd-Moser (KAM) theorem [2]. For sufficiently small nonlinear coupling (small in the sense that the nonlinear energy in the chain is small compared to the linear energy in the chain) the KAM theorem asserts that phase space trajectories for almost all initial conditions will be constrained to lie on N-dimensional tori rather than be free to wander over the full $(2N-1)$-dimensional energy surface. As the nonlinear coupling is increased the tori are destroyed so that an increasing fraction of the energy surface is accessible. For sufficiently large nonlinear coupling all tori are destroyed and the phase space trajectory will wander freely over the energy surface.

Quantitative algebraic results for the above numerical experiments rely on a detailed analysis of the coupling between the harmonic modes together with the employment of perturbation methods. This program has been carried out most comprehensively in the case where energy is initially supplied to the lowest-frequency harmonic mode. Here accurate estimates have been obtained for FPU periods and also for FPU superperiods using a shifted frequency perturbation analysis [6,7]. The most comprehensive algebraic study of the induction phenomenon to date is that of Saitô, Hirotomi, and Ichimura [4] based on a Mathieu function stability analysis. We are not aware of any previous algebraic studies of the induction time.

In this paper we have reexamined the induction phenomenon in quartic FPU chains. We show that estimates for the onset of induction based on Mathieu function stability analysis, while correctly reproducing the exponential growth of the mode energies, does not correctly identify the dominant modes. An analysis using a shifted frequency perturbation scheme and the analysis of mode resonances is presented. This analysis provides good agreement with numerical simulations for the pattern of mode excitation and for the identification of the dominant modes in the induction process. However, the analysis does not explain the exponential growth of mode energies.

In Sec. II the model Hamiltonian and the equations of motion for the quartic FPU chain are presented. In Sec. III the explanation for the induction phenomenon using the Mathieu function stability analysis is reviewed and compared with numerical results. The shifted frequency perturbation analysis is presented in Sec. IV. The possibility of reduction of order due to near resonances is examined in Sec. V for the $N=15$ particle chain. It is found that the first such reduction of order is due to a near resonance between the initially excited mode 11 and modes 9 and 13. Modes 9 and 13 are also found to be the dominant modes in numerical simulations of the induction phenomenon in the $N=15$ particle

chain. A generic near resonance in the induction phenomenon in quartic chains of length N is identified in Sec. VI. Numerical simulations reveal that the modes involved in the generic near resonance are the dominant modes in the induction process. The paper concludes with a summary and discussion in Sec. VII.

II. QUARTIC FPU CHAIN: MODEL EQUATIONS

The Hamiltonian for a quartic FPU chain with fixed ends and N free moving particles is

$$H=\frac{1}{2}\sum_{n=1}^{N}(\dot{x}_n)^2+\frac{1}{2}\sum_{n=0}^{N}(x_{n+1}-x_n)^2+\frac{\beta}{4}\sum_{n=0}^{N}(x_{n+1}-x_n)^4, \tag{2.1}$$

where x_i denotes the amplitudes of the ith particle from its equilibrium position, $x_0=x_{N+1}=0$, and β is the nonlinear coupling parameter. It is convenient to introduce normal mode coordinates

$$q_s(t)=\sqrt{\frac{2}{N+1}}\sum_{n=1}^{N}x_n(t)\sin\left(\frac{n\pi s}{N+1}\right), \quad s=1,2,\ldots,N \tag{2.2}$$

and

$$\omega_s=2\sin\left(\frac{\pi s}{2(N+1)}\right) \tag{2.3}$$

so that the Hamiltonian can be rewritten as

$$H=\frac{1}{2}\sum_{s=1}^{N}(\dot{q}_s^2+\omega_s^2q_s^2)+\frac{\beta}{8(N+1)}\sum_{s=1}^{N}\sum_{s'=1}^{N}\sum_{s''=1}^{N}\sum_{s'''=1}^{N}A_{s,s',s'',s'''}q_sq_{s'}q_{s''}q_{s'''}, \tag{2.4}$$

where

$$\begin{aligned}A_{s,s',s'',s'''}=\omega_s\omega_{s'}\omega_{s''}\omega_{s'''}[&B(s+s'+s''+s''')\\&+B(s-s'+s''+s''')+B(s+s'-s''+s''')\\&+B(s+s'+s''-s''')+B(s-s'-s''+s''')\\&+B(s-s'+s''-s''')+B(s+s'-s''-s''')\\&+B(s-s'-s''-s''')]\end{aligned} \tag{2.5}$$

and

$$B(r)=\begin{cases}1 & \text{for } r=0\\ -1 & \text{for } r=\pm 2(N+1)\\ 0 & \text{otherwise.}\end{cases} \tag{2.6}$$

In the normal mode representation (2.4), the harmonic Hamiltonian ($\beta=0$) is a sum of N independent harmonic oscillators with amplitudes q_s and frequencies ω_s. The normal mode representation of the FPU Hamiltonian, (2.4) is thus a convenient form for perturbation studies with β as the perturbation parameter.

The equation of motion for mode s of a quartic FPU chain is

$$\ddot{q}_s=-\omega_s^2q_s-\frac{\beta}{2(N+1)}\sum_{s'=1}^{N}\sum_{s''=1}^{N}\sum_{s'''=1}^{N}[A_{s,s',s'',s'''}q_{s'}q_{s''}q_{s'''}] \tag{2.7}$$

or, equivalently,

$$\begin{aligned}\ddot{q}_s=-\omega_s^2q_s-\frac{\beta}{2(N+1)}\Bigg[&q_s^3A_{s,s,s,s}+3q_s^2{\sum_{s'=1}^{N}}'A_{s,s,s,s'}q_{s'}\\&+3q_s{\sum_{s'=1}^{N}}'{\sum_{s''=1}^{N}}'A_{s,s,s',s''}q_{s'}q_{s''}\\&+{\sum_{s'=1}^{N}}'{\sum_{s''=1}^{N}}'{\sum_{s'''=1}^{N}}'A_{s,s',s'',s'''}q_{s'}q_{s''}q_{s'''}\Bigg],\end{aligned} \tag{2.8}$$

where the primes on the summation signs in Eq. (2.8) indicate that the summations do not include the index s. It readily follows from Eq. (2.8) that an initially quiescent mode s may become excited by modes s',s'',s''' (not necessarily all distinct) provided the amplitudes of these modes is nonzero and the coefficient $A_{s,s',s'',s'''}$ is nonzero. This is an example of a mode selection rule. The full list of nonzero coefficients $A_{s,s',s'',s'''}$ for the quartic FPU chain with $N=15$ moving particles and two end particles held fixed is tabulated in [5]. A complete account of mode selection rules for quartic FPU chains has been presented in [8].

III. INDUCTION PHENOMENON

The induction phenomenon was reported [3] in a numerical study of a quartic FPU chain with $N=15$ free particles and two end particles held fixed. In this study energy was initially supplied to mode $s=11$ via the initial conditions

$$q_s(0)=\begin{cases}2 & \text{for } s=11\\ 0 & \text{for } s\neq 11\end{cases} \tag{3.1}$$

and

$$\dot{q}_s(0)=0 \quad \text{for all } s. \tag{3.2}$$

Simulations were carried out over a range of values of the nonlinear coupling β and energy was found to remain essentially in the initially excited mode until after the elapse of an induction time when it was transferred abruptly to the other (odd) modes of the system. It follows from the selection rules [8] that the even modes cannot be excited by the initial excitation of an odd mode.

An explanation for the induction phenomenon was subsequently provided in [4]. This explanation was based on an analysis of the mode selection rules leading to a reduced set of decoupled linear mode equations [9]

$$\ddot{q}_s=-\omega_s^2q_s-\frac{3\beta}{16}\omega_s^2\omega_{11}^2q_sq_{11}^2, \tag{3.3}$$

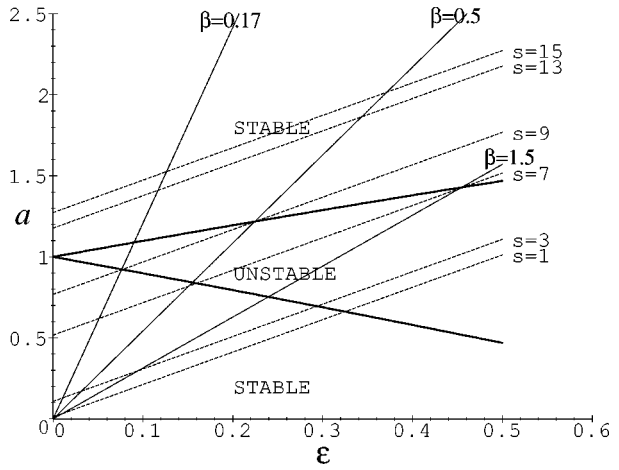

FIG. 1. Mode stability based on the Mathieu function analysis. The stable and unstable regions are demarked by thick lines, Eq. (3.8). The dashed lines are stability lines for the modes at arbitrary β and the solid lines are stability lines for a given β but arbitrary mode. The stability of a mode is determined by the region in which the stability lines intersect.

with q_{11} approximated by the harmonic solution $2\cos(\omega_{11}t)$. This reduced set was transformed into the canonical form of Mathieu's equation

$$q_s''+[a_s+2\epsilon_s\cos(2\tau)]q_s=0 \tag{3.4}$$

by defining

$$\tau=\omega_{11}, \tag{3.5}$$

$$a_s=\left(\frac{\omega_s}{\omega_{11}}\right)^2+\frac{3\beta\omega_s^2}{8}, \tag{3.6}$$

$$\epsilon_s=\frac{3\beta\omega_s^2}{16}. \tag{3.7}$$

The stability of the modes was then deduced using standard results for Mathieu's equation [10]. In particular, the solutions of Mathieu's equation are unstable for

$$1-\epsilon_s-\frac{1}{8}\epsilon_s^2+O(\epsilon_s^3)\leqslant a_s\leqslant 1+\epsilon_s-\frac{1}{8}\epsilon_s^2+O(\epsilon_s^3), \tag{3.8}$$

$$4-\frac{1}{12}\epsilon_s^2+O(\epsilon_s^3)\leqslant a_s\leqslant 4+\frac{5}{12}\epsilon_s^2+O(\epsilon_s^3). \tag{3.9}$$

The stability of a given mode can be determined graphically by using Eqs. (3.6) and (3.7) to plot a_s versus ϵ_s for (i) each mode s with β arbitrary and (ii) fixed β but arbitrary mode s. If the intersection of these two lines lies in the stable (unstable) regime as determined by Eqs. (3.8) and (3.9), then mode s is deemed to be stable (unstable) for the fixed value of β (see Fig. 1). It was concluded that the energy of the unstable modes would grow most rapidly and trigger the transfer of energy to other modes. As evidence in favor of this analysis, Saitô, Hirotomi, and Ichimura reported that mode 9 was the first to obtain energy comparable to the initially excited mode for $\beta=0.5$ and mode 9 was the only mode deemed to be unstable in the stability analysis for this value of β.

We have carried out a comprehensive comparison between predictions of the stability analysis and numerical simulations and we find that the stability analysis does not correctly identify the dominant modes involved in the induction process over the range of $\beta\in[0.1,1.0]$. The main predictions of the stability analysis within this range may be summarized as follows (see Fig. 1): (i) For $0.1<\beta<0.17$, all modes are stable; (ii) for $0.17<\beta\leqslant 0.5$, all modes are stable except for mode 9; (iii) for $0.5<\beta<1.0$, all modes are stable except for mode 7.

In extensive numerical simulations over a range of β we have numerically integrated the particle equations of motion, with initial conditions from Eqs. (3.1) and (3.2), and we have made plots of the mode energy versus time. Some sample plots are shown in Figs. 2, 3, and 4 for $\beta=0.15$, 0.3, and 0.7. The results of the numerical simulations reveal uniform patterns of behavior across a range of $\beta\in[0.1,1.0]$ as follows.

(i) In the early part of the simulations (Fig. 2) the energy in the modes is ordered

$$E_{11}>E_1>E_9>E_{13}>E_3>E_7>E_{15}>E_5. \tag{3.10}$$

(ii) The energy in mode 1 and mode 11 remains approximately constant until the onset of induction. (iii) The energy in all modes except mode 1 and mode 11 grows on average at an approximately exponential rate until the onset of induction (Fig. 3). (iv) After the first ten or so model time units the energy in modes 9 and 13 is comparable and these two modes are the first modes to attain energy comparable to the initially excited mode (Fig. 4). (v) The induction time increases with decreasing β (Fig. 4).

IV. SHIFTED FREQUENCY ANALYSIS

The discrepancies between the theoretical predictions and the numerical simulations in the preceding section reveal that the reduced set of decoupled linear mode equations (3.3) do not adequately describe the dynamics of the modes in the induction phenomenon. One of the reasons for this failure is that the approximation of Eq. (3.3) is not a consistent truncation of the mode equations. In particular, Eq. (3.3) includes some of the multinomial terms of the form $q_s q_{11}^2$ that are permitted by the selection rules but omits others. A more complete set of equations including all such multinomial terms would not be decoupled and could not be reduced to Mathieu equations.

The shifted frequency perturbation scheme provides a consistent truncation of the mode equations up to a cutoff order. We have employed this scheme here to investigate energy sharing in the full set of coupled mode equations, (2.7) for the $(15+2)$-particle chain initially excited in mode 11. This scheme, which is essentially a generalization of the Poincaré-Lindstedt method to systems with many degrees of freedom, has been used previously to explain periodic energy exchanges in FPU chains [11–14,6,7]. In this scheme it is assumed that the mode amplitudes as well as the mode frequencies can be formally expanded as power series in β. These expansions are written

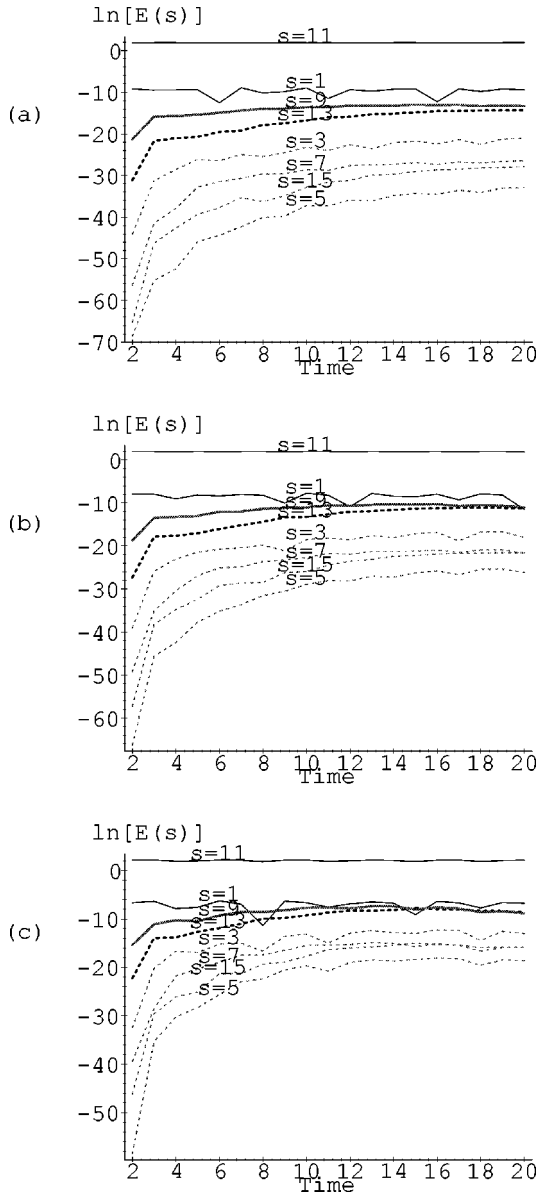

FIG. 2. Plots of the logarithm of the mode energy versus time in the early part of the simulation for three different values of β: (a) $\beta=0.15$, (b) $\beta=0.3$, and (c) $\beta=0.7$.

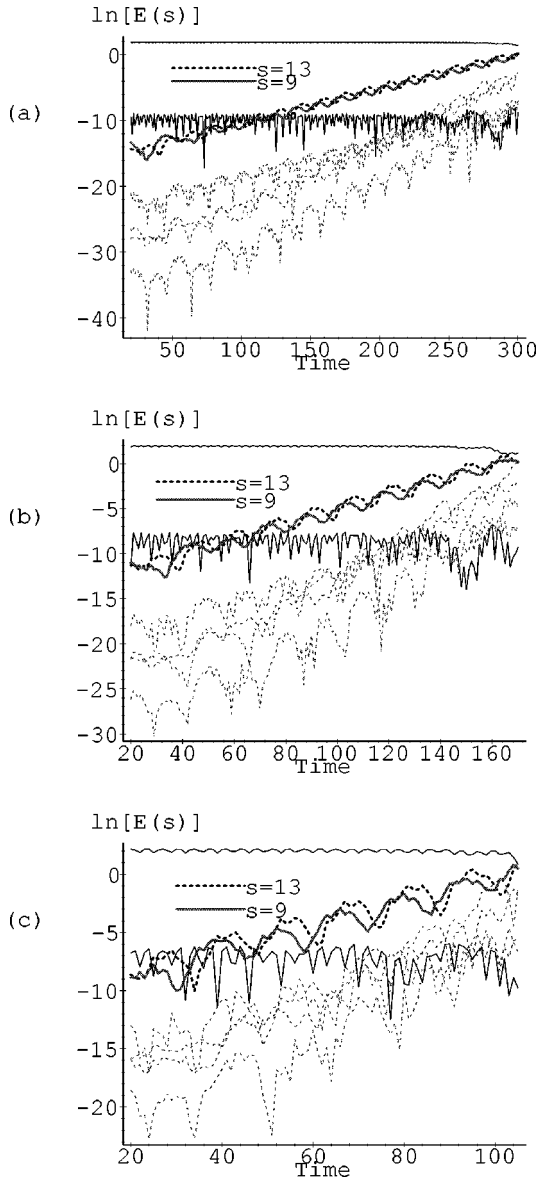

FIG. 3. Plots of the logarithm of the mode energy versus time for times up to the onset of induction for three different values of β: (a) $\beta=0.15$, (b) $\beta=0.3$, and (c) $\beta=0.7$. Note the different time scale in the plots.

$$q_s=q_{s,0}+\beta q_{s,1}+\beta^2 q_{s,2}+\cdots, \tag{4.1}$$

$$\omega_s^2=\Omega_s^2-\beta\mu_{s,1}-\beta^2\mu_{s,2}-\cdots, \tag{4.2}$$

where Ω are the shifted frequencies of the oscillators and μ are the frequency shifts. In the standard shifted-frequency perturbation scheme the mode-amplitude expansions are substituted into the equations of motion (2.7) and the frequency expansions are substituted into the linear terms in this equation. The coefficients of equal powers of β are then equated in the resultant equations. This yields N equations of motion (one for each mode) at each order n of the form

$$q_{s,n}+\Omega_s^2 q_{s,n}=\left[\sum_{p=1}^{n}\mu_{s,p}q_{s,n-p}\right]-F_{n-1}, \tag{4.3}$$

where the forcing term F_{n-1} comprises all the $(n-1)$th-order terms inside the square brackets on the right-hand side of Eq. (2.7). The forcing term is zero unless the following conditions are met:

$$A_{s,s',s'',s'''}q_{s'}q_{s''}q_{s'''}\neq 0, \tag{4.4}$$

$$q_{s'}q_{s''}q_{s'''}=O(n-1). \tag{4.5}$$

The resultant equations with initial conditions

$$q_{11,0}(0)=2, \tag{4.6}$$

$$q_{s,0}(0)=0 \quad \forall\ s\neq 11, \tag{4.7}$$

$$q_{s,j}(0)=0 \quad \forall\ s, \quad \forall\ j\geq 1, \tag{4.8}$$

$$\dot{q}_{s,j}(0)=0 \quad \forall\ s,j \tag{4.9}$$

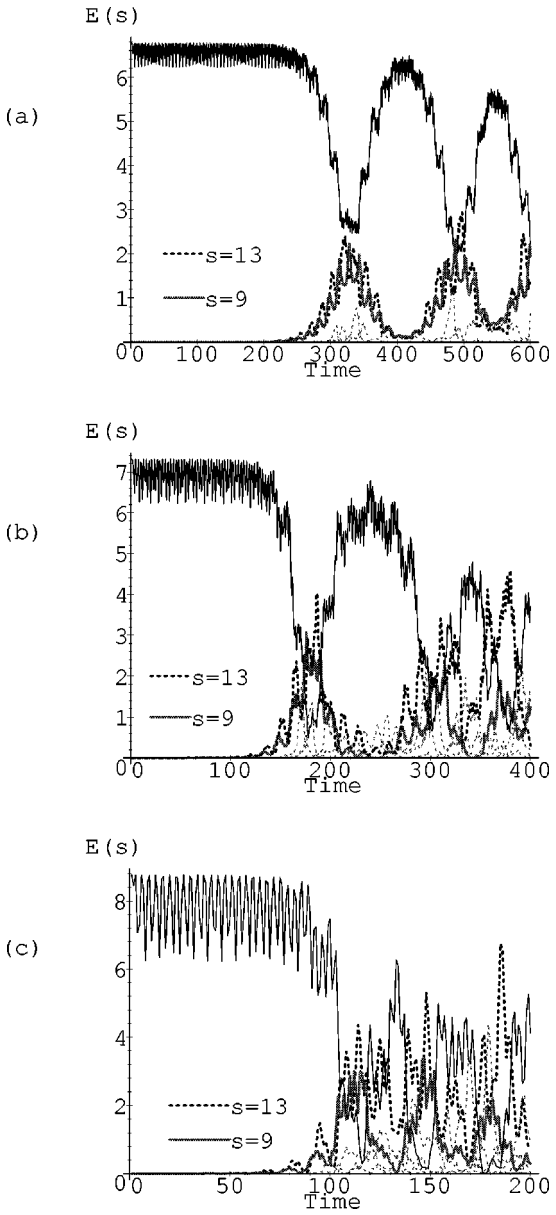

FIG. 4. Plots of the mode energy versus time for times extending beyond the induction time for three different values of β: (a) $\beta=0.15$, (b) $\beta=0.3$, and (c) $\beta=0.7$. Note the different time scale in the plots.

can be solved explicitly by proceeding order by order up to a cutoff order. The frequency shifts are defined so as to remove secular terms from the solutions.

The zeroth order equations are

$$\ddot{q}_{s,0}+\Omega_s^2 q_{s,0}=0, \tag{4.10}$$

with solutions

$$q_{11,0}=2\cos(\Omega_{11}t), \tag{4.11}$$

$$q_{s,0}=0 \quad \forall\ s\neq 11. \tag{4.12}$$

The dual requirement that $A_{s,s',s'',s'''}$ is nonzero and $q_{s'}q_{s''}q_{s'''}$ is a nonzero term of order zero only permits forcing terms in the first-order equations for modes $s=1$ via

$$A_{1,11,11,11}q_{11,0}^3\neq 0 \tag{4.13}$$

and $s=11$ via

$$A_{11,11,11,11}q_{11,0}^3\neq 0. \tag{4.14}$$

Thus mode 1 is the only additional mode to become excited at this order. The first-order equations can be written in the form

$$\ddot{q}_{11,1}+\Omega_{11}^2 q_{11,1}=\left(2\mu_{11,1}-\frac{9}{16}\omega_{11}^4\right)\cos(\Omega_{11}t) - \frac{3}{16}\omega_{11}^4\cos(3\Omega_{11}t), \tag{4.15}$$

$$\ddot{q}_{1,1}+\Omega_1^2 q_{1,1}=\frac{3}{16}\omega_1\omega_{11}^3\cos(\Omega_{11}t)+\frac{1}{16}\omega_1\omega_{11}^3\cos(3\Omega_{11}t), \tag{4.16}$$

$$\ddot{q}_{s,1}+\Omega_s^2 q_{s,1}=0, \quad s=3,5,7,9,13,15. \tag{4.17}$$

Equation (4.15) contains a resonance term that would lead to secular terms in the solution. This secular term is eliminated by defining the frequency shift

$$\mu_{11,1}=\frac{9}{32}\omega_{11}^4. \tag{4.18}$$

No other frequency shifts are defined at this order. It is a simple matter to obtain solutions to Eqs. (4.15)–(4.17) subject to the initial conditions (4.6)–(4.9). Explicitly,

$$q_{1,1}=\frac{\omega_1\omega_{11}^3}{4}\left[(7\Omega_{11}^2-\Omega_1^2)\cos(\Omega_1 t)+\left(\frac{3}{4}\Omega_1^2-\frac{27}{4}\Omega_{11}^2\right)\times\cos(\Omega_{11}t)+\left(\frac{1}{4}\Omega_1^2-\frac{1}{4}\Omega_{11}^2\right)\cos(3\Omega_{11}t)\right]\times(\Omega_1^4-10\Omega_1^2\Omega_{11}^2+9\Omega_{11}^4)^{-1}, \tag{4.19}$$

$$q_{11,1}=\frac{3\omega_{11}^2}{128\Omega_{11}^2}[\cos(\omega_{11}t)+\cos(3\omega_{11}t)], \tag{4.20}$$

$$q_{s,1}=0 \quad \text{for } s=3,5,7,9,13,15. \tag{4.21}$$

At second order, the dual requirement that $A_{s,s',s'',s'''}$ is nonzero and $q_{s'}q_{s''}q_{s'''}$ is a nonzero term of order one only permits forcing terms in the equations for modes $s=1,9,11$ via

$$A_{1,11,11,11}q_{11,0}q_{11,0}q_{11,1}\neq 0, \tag{4.22}$$

$$A_{1,11,11,1}q_{11,0}q_{11,0}q_{1,1}\neq 0, \tag{4.23}$$

$$A_{9,1,11,11}q_{1,1}q_{11,0}q_{11,0}\neq 0, \tag{4.24}$$

$$A_{11,11,11,11}q_{11,0}q_{11,0}q_{11,1}\neq 0, \tag{4.25}$$

$$A_{11,11,11,1}q_{11,0}q_{11,0}q_{1,1}\neq 0. \tag{4.26}$$

TABLE I. All the nonvanishing forcing terms in the mode equations of motion for the newly excited mode at each order in the shifted frequency perturbation treatment (see Sec. IV).

First order	Second order	Third order	Fourth order	Fifth order	Sixth order	Seventh order
$A_{1,11,11,11}$	$A_{9,11,11,1}$	$A_{13,11,1,1}$	$A_{3,11,11,13}$	$A_{7,11,1,13}$	$A_{15,11,1,3}$	$A_{5,11,9,3}$
$q_{11,0}q_{11,0}q_{11,0}$	$q_{11,0}q_{11,0}q_{1,1}$	$q_{11,0}q_{1,1}q_{1,1}$	$q_{11,0}q_{11,0}q_{13,3}$	$q_{11,0}q_{1,1}q_{13,3}$	$q_{11,0}q_{1,1}q_{3,4}$	$q_{11,0}q_{9,2}q_{3,4}$
		$A_{13,11,11,9}$	$A_{3,1,1,1}$	$A_{7,11,11,3}$	$A_{15,1,1,13}$	$A_{5,9,9,9}$
		$q_{11,0}q_{11,0}q_{9,2}$	$q_{1,1}q_{1,1}q_{1,1}$	$q_{11,0}q_{11,0}q_{3,4}$	$q_{1,1}q_{1,1}q_{13,3}$	$q_{9,2}q_{9,2}q_{9,2}$
			$A_{3,11,1,9}$	$A_{7,11,9,9}$	$A_{15,1,9,9}$	$A_{5,1,1,3}$
			$q_{11,0}q_{1,1}q_{9,2}$	$q_{11,0}q_{9,2}q_{9,2}$	$q_{1,1}q_{9,2}q_{9,2}$	$q_{1,1}q_{1,1}q_{3,4}$
				$A_{7,1,1,9}$	$A_{15,11,9,13}$	$A_{5,1,9,13}$
				$q_{1,1}q_{1,1}q_{9,2}$	$q_{11,0}q_{9,2}q_{13,3}$	$q_{1,1}q_{9,2}q_{13,3}$
						$A_{5,11,13,13}$
						$q_{11,0}q_{13,3}q_{13,3}$

Thus mode 9 is the only additional mode to be excited at second order.

At each order one new mode becomes excited until at seventh order all odd modes are active. Table I lists all nonvanishing forcing terms in the equations of motion for the newly excited mode at each order. The order of appearance of the remaining modes is mode 13 at third order, mode 3 at fourth order, mode 7 at fifth order, mode 15 at sixth order, and finally mode 5 at seventh order. This order of appearance of the modes in the shifted-frequency perturbation scheme matches precisely with the ordering of the modes according to mode energy in the early part of the numerical simulations (see Fig. 2).

In general, the equation of motion for mode s at order $j \geqslant j^*(s)$ [where $j^*(s)$ is the order at which mode s becomes excited] may be written in the form

$$\ddot{q}_{s,j}+\Omega_s^2 q_{s,j}=\sum_{k=1}^{j} \mu_{s,k} q_{s,j-k}+\sum_{l} \alpha_l(s,j)\cos[\nu_l(s,j)t], \tag{4.27}$$

where the $\nu_l(s,j)$ are linear combinations of the shifted frequencies Ω and the number of terms in the sum over l depends on the mode s and the order j. In the particular case $j=j^*(s)$, the mode amplitudes $q_{s,j-k}=0$ and the solution of Eq. (4.27) corresponding to initial conditions (4.6)–(4.9) is

$$q_{s,j^*}=\sum_{l} \frac{\alpha_l(s,j^*)}{\Omega_s^2-\nu_l^2(s,j^*)}[\cos\ \nu_l(s,j^*)t-\cos\ \Omega_s t]. \tag{4.28}$$

At the next order $j=j^*+1$, the equation of motion for mode s is

$$\ddot{q}_{s,j^*+1}+\Omega_s^2 q_{s,j^*+1}=\mu_{s,1} q_{s,j^*}+F_{j^*}. \tag{4.29}$$

At this order the governing equation always contains a forcing term via

$$A_{s,s,11,11} q_{s,j^*} q_{11,0} q_{11,0} \neq 0. \tag{4.30}$$

This particular forcing term has a resonance component since

$$q_{11,0}^2=2+2\cos(2\Omega_{11}t). \tag{4.31}$$

Excluding the case $s=11$, the resonance term is removed by defining

$$\mu_{s,1}=\frac{3\beta}{(N+1)}A_{s,s,11,11}, \tag{4.32}$$

where the further factor 3 is obtained from the three permutations of the forcing [Eq. (4.30)] arising from the sum in Eq. (2.7). Finally, using Eqs. (2.5) and (2.6) with $N=11$, the first-order frequency shifts for all modes other than the initially excited mode [see Eq. (4.18)] are obtained:

$$\mu_{s,1}=\begin{cases} 3\omega_s^2\omega_{11}^2/8 & \text{for } s\neq 5,11 \\ 3\omega_5^2\omega_{11}^2/16 & \text{for } s=5. \end{cases} \tag{4.33}$$

It is not possible to explicitly obtain higher-order frequency corrections for all modes without first obtaining explicit solutions to the mode equations at order j^*. We have obtained explicit solutions up to second order. The only additional frequency shift to be resolved up to this order is

$$\mu_{11,2}=-\frac{27\omega_{11}^8}{8192\Omega_{11}^2}+\frac{123\omega_{11}^6\omega_1^2\Omega_{11}^2}{512\Omega_1^4-5120\Omega_1^2\Omega_{11}^2+4608\Omega_{11}^4} -\frac{15\omega_{11}^6\omega_1^2\Omega_1^2}{512\Omega_1^4-5120\Omega_1^2\Omega_{11}^2+4608\Omega_{11}^4}. \tag{4.34}$$

V. RESONANCE MECHANISM IN INDUCTION: $N=15$

It can be readily seen from Eq. (4.28) that the dominant contribution to an initially excited mode comes from near resonances

$$\Omega_s \approx \nu_l(s,j^*). \tag{5.1}$$

In particular, if $\Omega_s^2-\nu_l^2(s,j^*)\approx O(\beta^n)$ then this reduces mode s to order j^*-n. The importance of the reduction of order via near resonances in mode energy sharing was pointed out by Ford and Waters [13] in a shifted frequency analysis of the FPU period. The first reduction of order in the induction phenomenon occurs for mode 13 at third order. From the entries in Table I it can be seen that one of the contributions to the forcing term in the equation for mode 13 at third order has frequency

$$\nu=2\Omega_{11}-\Omega_9. \tag{5.2}$$

This term results in a near resonance since

$$\Omega_{11}\approx(\Omega_9+\Omega_{13})/2. \tag{5.3}$$

Other near resonances occur, but at higher orders. For example, the primary near resonance responsible for the FPU period in the quartic chain is between modes 1 and 3. This near resonance occurs at second order in the shifted frequency analysis of the FPU period [7] but at fourth order in the shifted frequency analysis with initial conditions for induction; cf. Table I.

The near resonance resulting in the growth of mode 13 at third order also appears in the equation for mode 9 at fourth order via

$$A_{9,11,11,13}q_{11,0}q_{11,0}q_{13,3}\neq 0. \tag{5.4}$$

This near resonance would be expected to be dominant in the induction process over a range of β for which

$$2\Omega_{11}-\Omega_9-\Omega_{13}\leqslant O(\beta^3). \tag{5.5}$$

Ideally, we would like to be able to calculate the frequency corrections up to third order (where this near resonance first appears in the mode equations); however, the rapid escalation of terms in the perturbation series has prevented us from going beyond first order in the frequency corrections except for mode $s=11$ [Eq. (4.34)]. At zeroth order the harmonic frequencies yield

$$2\Omega_{11}-\Omega_9-\Omega_{13}\approx 0.068, \tag{5.6}$$

whereas the shifted frequencies with first-order corrections yield an exact resonance for $\beta\approx 0.154$. Whether or not higher-order corrections yield an exact resonance or a near resonance is not vital to the analysis since the solutions for the mode energies with exact resonances are similar to the solutions with near resonances over time scales $t<2\pi/[(2\Omega_{11}-\Omega_9)-\Omega_{13}]$. Thus, over these times we anticipate that the solution for $q_{13}(t)$ will contain a (near) secular term $\sim t\,\sin(\Omega_{13}t)$ at third order and the solution for $q_9(t)$ will contain a (near) secular term $\sim t\,\sin(\Omega_{13}t)$ at fourth order. The associated mode energies resulting from these (near) resonance terms can grow rapidly in time depending on the closeness of the near resonance. This resonance analysis suggests that modes 9 and 13 will play a dominant role in energy transfers precipitating the induction phenomenon. In numerical experiments of the induction phenomenon in the $N=15$ particle chain over a range of $\beta\in[0.1,1]$ it is observed that (apart from the initially excited mode) modes 9 and 13 are always the dominant modes. Hence the resonance mechanism correctly identifies the dominant modes, but it does not explain the exponential growth of energy in these modes that is observed in numerical simulations.

VI. GENERIC RESONANCE MECHANISM IN INDUCTION: ARBITRARY N

In the $N=15$ particle chain the induction phenomenon is characterized by (i) a stable exchange of energy between the initially excited mode, mode 11, and the lowest frequency mode, mode 1, and (ii) an unstable exchange of energy between modes 11, 9, and 13. In the early part of simulations the energy is ordered $E_{11}>E_1>E_9>E_{13}$. Induction then takes place when $E_{11}\approx E_9\approx E_{13}$, which is greater than the energy in all other modes. The initial transfer of energy from mode 11 to mode 1 is an immediate consequence of the selection rules. The ordering of mode energies in the early part of simulations was explained in the above using the mode selection rules and perturbation analysis. The simultaneous growth of energy in modes 9 and 13 as the dominant growing modes in the induction process was then explained on the basis of a near resonance between modes 11, 9, and 13.

In this section we hypothesize generic conditions for induction involving a generic resonance in chains of arbitrary length N. The condition that the initially excited mode s_0 first excites mode 1 is met if

$$s_0\pm s_0\pm s_0\pm 1=\begin{cases}\pm 2(N+1)\\ 0,\end{cases} \tag{6.1}$$

which implies either

$$s_0^+=\frac{2(N+1)+1}{3} \tag{6.2}$$

or

$$s_0^-=\frac{2(N+1)-1}{3}, \tag{6.3}$$

provided s_0 is an integer. At second order in a shifted-frequency perturbation analysis a further mode can then be excited via

$$A_{s_2,s_0,s_0,1}q_{s_0,0}q_{s_0,0}q_{1,1}\neq 0. \tag{6.4}$$

It follows from Eqs. (2.5) and (2.6) that

$$s_2=\begin{cases}s_0+2 & \text{if } s_0=s_0^-\\ s_0-2 & \text{if } s_0=s_0^+.\end{cases} \tag{6.5}$$

At third order mode s_3 can be excited via

$$A_{s_3,s_0,s_0,s_2}q_{s_0,0}q_{s_0,0}q_{s_2,2}\neq 0. \tag{6.6}$$

It follows from Eqs. (2.5), (2.6), and (6.5) that

$$s_3=\begin{cases}s_0-2 & \text{if } s_0=s_0^-\\ s_0+2 & \text{if } s_0=s_0^+.\end{cases} \tag{6.7}$$

TABLE II. Dominant modes according to the generic resonance mechanism in the induction phenomenon (see Sec. VI) for chains of different length N. Also shown is the zeroth-order approximation of the closeness of the near resonance, Eq. (6.11).

N	7	9	10	12	13	15	16	18	19
s_0	5	7	7	9	9	11	11	13	13
s_2	7	5	9	7	11	9	13	11	15
s_3	3	9	5	11	7	13	9	15	11
$\Delta\Omega$	0.25	0.17	0.14	0.10	0.085	0.068	0.057	0.050	0.042

Since s_2 and s_3 are (odd) modes with frequencies closest to and on either side of the initially excited mode s_0 it is anticipated that there will be a generic near resonance arising from

$$2\Omega_{s_0} \approx \Omega_{s_2} + \Omega_{s_3}. \tag{6.8}$$

Thus we have generic conditions for induction. Note that near resonance terms will be ubiquitous in quartic chains due to interactions arising from nonvanishing coefficients of the form $A_{s-2,s,s,s+2}$. In general, these resonances will occur at higher orders in the perturbation analysis. If these near resonances are sufficiently close then they too will lead to large-scale energy sharing.

In summary, if a quartic chain of N particles is initially excited in mode s_0 according to Eqs. (6.2) and (6.3) then this will in turn first excite mode 1 (at first order in a shifted frequency perturbation treatment). The two modes s_0 and s_1 will subsequently excite the two odd frequency modes with frequencies closest to the initially excited mode at second order [Eq. (6.5)] and third order [Eq. (6.7)]. The equation of motion for mode s_3 at third order will contain a near resonance term with frequency

$$2\Omega_{s_0} - \Omega_{s_2}. \tag{6.9}$$

A similar near resonance term with frequency

$$2\Omega_{s_0} - \Omega_{s_3} \tag{6.10}$$

will then appear in the equation of motion for mode s_2 at fourth order. If the near resonance is sufficiently close then this will lead to the growth of modes s_2 and s_3 resulting in induction.

According to the generic mechanism for induction described above, induction cannot occur in chains with $N = 3n+2$ particles (n is any natural number) and induction cannot occur in a chain with $N<7$. Table II contains a list of

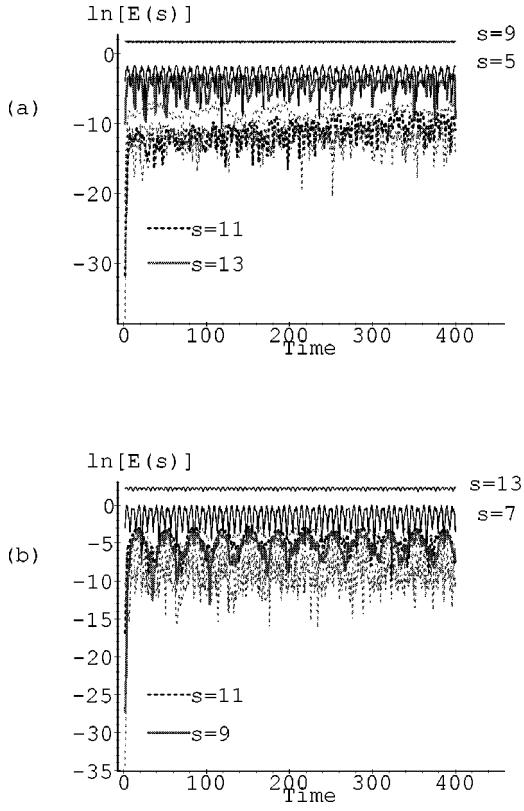

FIG. 5. Plots of the logarithm of the mode energy versus time for an $N=15$ particle chain initially excited in mode (a) $s_0=9$ and (b) $s_0=13$, with $\beta=0.7$.

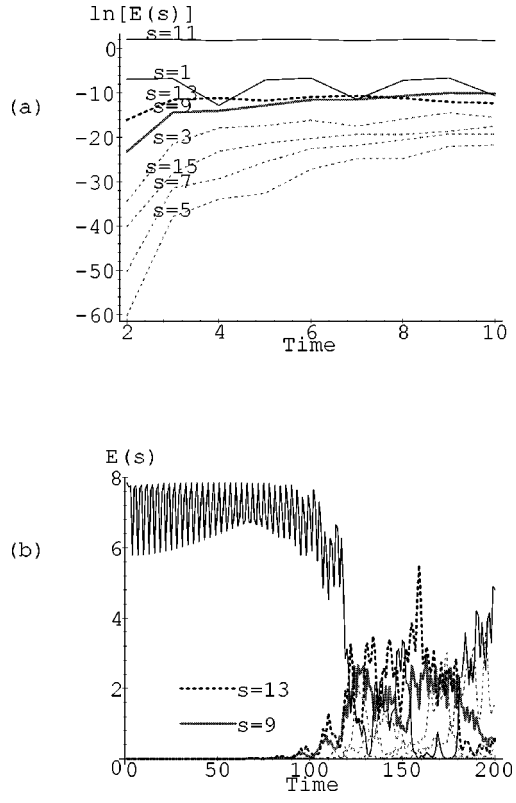

FIG. 6. Plots of (a) the logarithm of the mode energy versus time in the early part of a simulation and (b) the mode energy versus time over a full simulation for an $N=16$ particle chain initially excited in mode $s_0=11$ with $\beta=0.7$.

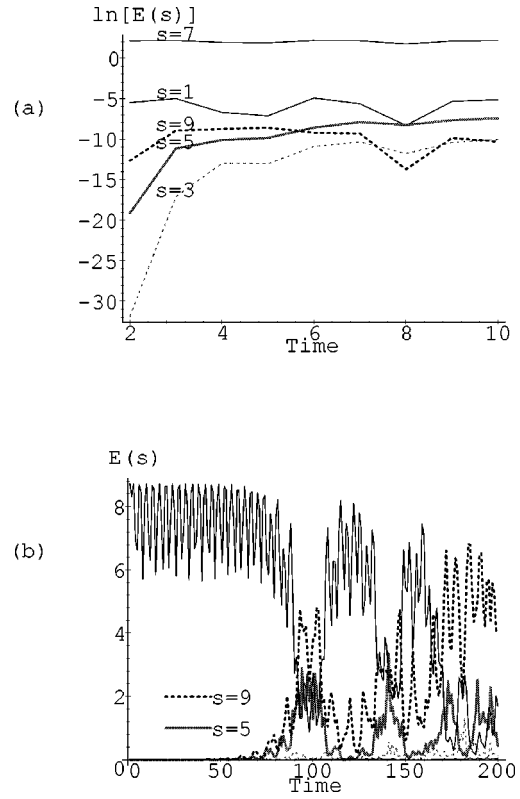

FIG. 7. Plots of (a) the logarithm of the mode energy versus time in the early part of a simulation and (b) the mode energy versus time over a full simulation for an $N=10$ particle chain initially excited in mode $s_0=7$ with $\beta=0.7$.

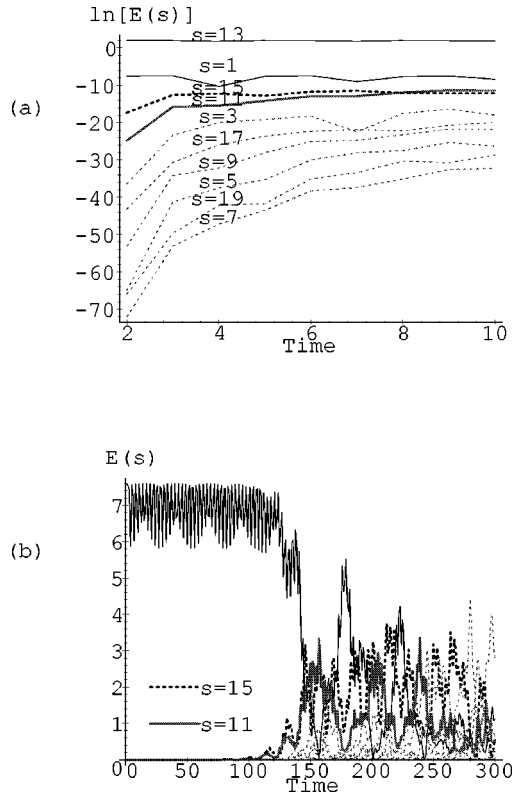

FIG. 8. Plots of (a) the logarithm of the mode energy versus time in the early part of a simulation and (b) the mode energy versus time over a full simulation for an $N=19$ particle chain initially excited in mode $s_0=13$ with $\beta=0.7$.

modes s_0, s_2, s_3 involved in the onset of induction according to the generic mechanism for $N=7,9,\ldots,19$. The quantity

$$\Delta\Omega = 2\omega_{s_0} - \omega_{s_2} - \omega_{s_3} \tag{6.11}$$

is also listed in Table II as a zeroth-order measure of the closeness of the near resonance.

We have carried out extensive numerical simulations of the quartic chain with different N and excited in different initial modes and the results are consistent with the generic mechanism for induction outlined above. Some of the results of the numerical simulations are shown in Figs. 5–8. In these simulations we have set the nonlinear coupling to $\beta=0.7$ and the initial conditions are of the form $q_s(0)=0$ and $\dot{q}_s(0)=0$ for all modes except mode s_0, where $q_{s_0}(0)=2$.

Figure 5 shows plots of the mode energies in a 15-particle chain initially excited in (a) mode 9 and (b) mode 13. The characteristic features of induction, an initial quiescent period followed by an abrupt transfer of energy to other modes, is not seen in either of these simulations (see further remarks below). Figure 6 shows plots of the mode energies in a 16-particle quartic chain initially excited in mode 11. In the early part of the simulation the energy is ordered $E_{11}>E_1>E_{13}>E_9$, in agreement with the ordering predicted by the selection rules and perturbation analysis as summarized in Table II. Furthermore, modes 11, 9, and 13 are the dominant modes at the onset of induction in this system, in agreement with the resonance mechanism for induction. Figure 7 shows a plot of the mode energies in a 10-particle quartic chain initially excited in mode 7. The ordering $E_7>E_1>E_9>E_5$ in the early part of the simulation and the dominance of modes 7, 9, and 5 at the onset of induction are consistent with the entries in Table II and the resonance mechanism for induction. Figure 8 shows induction in a 19-particle chain initially excited in mode 13. Again, the initial ordering $E_{13}>E_1>E_{15}>E_{11}$ and the dominance of modes 13, 15, and 11 at the onset of induction are consistent with the entries in Table II and the resonance mechanism.

The shortest quartic chain for which we could numerically obtain induction with the initial conditions above is the ($N=10$)-particle chain excited in mode 7 (Fig. 7). In particular, we did not observe induction in the ($N=9$)-particle chain excited in mode 7 or the ($N=7$)-particle chain excited in mode 5. One possible reason for this is that the near resonances involving modes 7, 5, and 9 in the ($N=9$)-particle chain and modes 5, 7, and 3 in the ($N=7$)-particle chain are not sufficiently close. Note that the closeness of the near resonance decreases with decreasing N, at least in the zeroth order approximation (Table II). Another possibility is that induction occurs but at much later times in these short chains. All of the numerical results that we have reported above have been restricted to times less than the time at which roundoff errors (as evidenced by the appearance of even modes) contaminate the results. It is possible to eliminate the spurious excitation of the even modes by integrating the particle equations of motion under the explicit restriction that $x_n=x_{N+1-n}$ and $\dot{x}_n=\dot{x}_{N+1-n}$, but this does not eliminate the possibility of roundoff errors. It is interesting to note in this connection that an apparent induction can be observed

in numerical simulations of the 15-particle chain initially excited in mode 9 for $\beta=1.5$ and initial conditions $q_s(0)=0$ and $\dot{q}_s(0)=0$ for all modes except $q_9(0)=2$. However, this apparent induction occurs as a result of significant growth of energy in the spurious mode 10. When we integrate the same system but with even modes set to zero no induction is observed even over much longer times. For the 15-particle chain initially excited in mode 9 we do expect widespread energy sharing for β sufficiently large, but we do not expect this energy sharing to follow the induction pattern of an initially quiescent period followed by abrupt energy sharing.

VII. SUMMARY AND DISCUSSION

In this paper we have reexamined the induction phenomenon in quartic Fermi-Pasta-Ulam chains that occurs when an initially excited mode transfers energy apparently abruptly to the other modes of the system after an initially quiescent induction time. This phenomenon has been studied extensively in previous work in the case of an $(N=15)$-particle chain initially excited in mode 11. The simulations of our present study demonstrate that the conclusions of the previous workers relating to the mechanism for induction are not correct. The Mathieu function stability analysis in previous work that was based on a reduced set of coupled mode equations was flawed because the reduced set did not include all of the significant mode interactions.

We carried out a shifted-frequency perturbation analysis of the quartic 15-particle chain with the initial conditions for induction and we found that the order of appearance of the modes in the perturbation analysis is consistent with the ordering of the modes according to the magnitude of their harmonic energies in the early part of simulations. We also identified a resonance mechanism to account for the dominant growing modes in the induction phenomenon. Finally, we identified a generic mechanism for induction in quartic FPU chains. In this generic mechanism an initially excited mode first excites mode 1 and then excites the two modes with frequencies closest to that of the initially excited mode (at second order and third order in the perturbation analysis). One of these modes has frequency less than the initially excited mode and the other has frequency greater than the initially excited mode. A near resonance term appears in the equations for these modes due to the fact that the frequency of the initially excited mode is essentially an average of the frequencies of these two neighboring modes. If the near resonance is sufficiently close then the energy in the neighboring modes can become comparable to the initially excited mode thus triggering induction.

The calculations in this study again support the usefulness of the shifted-frequency perturbation scheme for studying mode energy transfers in FPU chains. There are, however, several questions that we have not been able to answer within this framework. Why is the energy in mode 1 stable under the conditions for induction? [It follows from Eq. (4.19) that at short times the energy in mode 1 does not depend on the perturbation parameter β.] Why is the energy exchange between modes sometimes periodic and sometimes stochastic after the onset of induction? Why do all mode energies (except mode 1 and the initially excited mode) grow exponentially in time in the induction phenomenon? Can a stability analysis be carried out on the mode energies (perhaps along the lines of a Mathieu function analysis generalized to coupled oscillators) on a reduced set of equations that includes all significant mode interactions?

ACKNOWLEDGMENT

We would like to thank Dr. Simon Watt for useful discussions.

[1] E. Fermi, J. Pasta, and S. Ulam, Los Alamos Scientific Laboratory Report No. LA1940, 1955 (unpublished) [reprinted in *Nonlinear Wave Motion*, Vol. 15 of *Lectures in Applied Mathematics*, edited by A. C. Newell (American Mathematical Society, Providence, 1974), p. 143].

[2] J. Ford, Phys. Rep. **213**, 272 (1992).

[3] N. Ooyama, H. Hirooka, and N. Saitô, J. Phys. Soc. Jpn. **27**, 815 (1969).

[4] N. Saitô, N. Hirotomi and A. Ichimura, J. Phys. Soc. Jpn **39**, 1931 (1975).

[5] B. I. Henry and J. Grindlay, Physica D **28**, 49 (1987).

[6] D. S. Sholl and B. I. Henry, Phys. Lett. A **159**, 21 (1991).

[7] D. S. Sholl and B. I. Henry, Phys. Rev. A **44**, 6364 (1991).

[8] R. L. Bivins, N. Metropolis, and J. R. Pasta, J. Comput. Phys. **12**, 65 (1973).

[9] The reduced equation for mode 5 is slightly different since $B(s+s+11+11)=0$ for $s\neq 5$ but $B(5+5+11+11)=-1$. The different form of the equation for mode 5 [replace β by $\beta/2$ in Eq. (3.3)] was not included in the analysis of [4].

[10] See, for example, R. Grimshaw, *Nonlinear Ordinary Differential Equations* (Chemical Rubber, Boca Raton, FL, 1993).

[11] J. Ford, J. Math. Phys. **2**, 387 (1961).

[12] E. A. Jackson, J. Math. Phys. **4**, 686 (1963).

[13] J. Ford and J. Waters, J. Math. Phys. **4**, 1293 (1963).

[14] J. Grindlay and A. Opie, J. Phys. C **10**, 947 (1977).